A Novel Low Cost Converter for Torque Boost Integrated Starter Generator

G. G. RAJA SEKHAR
Associate Prof, Power Electronics & Electrical Drives,
Department of Electrical and Electronics Engineering,
KKR &KSR Institute of Tech & Sciences, Guntur-A.P, India
e-mail: rsgg73@gmail.com

B. Basava Raja
Professor & Head of the Department,
Department of Electrical and Electronics Engineering,
Gitam university Hyd campus (A.P), India.
e-mail: banakara36@gmail.com

Abstract- **New consumer requirements to modern cars have resulted in developing an integrated starter generator. This multifunctional and multi connected system is of great interest for commercial application. The integration of the internal combustion engine, the starter and the generator into a single power unit allows one to implement qualitatively a new concept of a car power unit with a substantial improvement of its ecological parameters. In this paper a novel low cost converter is proposed to extend the torque speed characteristics of Integrated Starter Generator (ISG). Finally Matlab/Simulink based model is developed and simulation results are presented.**

Keywords- Starter motor, Generator, IC Engine, Battery Pack.

I. INTRODUCTION

Due to the growing concerns on environment protection and energy conservation, the development of energy-efficient technologies for hybrid electric vehicles (HEVs) has taken on an accelerated pace [1]–[3]. Electric machines and drives are one of the key energy-efficient technologies for HEVs [4]–[6]. In a conventional automotive electrical system, because most of the electric machines cannot offer high starting torque and wide speed range simultaneously, the starter motor and the generator have to be separately employed for engine cranking and battery charging, respectively [7], [8].With the advancement of electric machines and power electronics technologies, the integrated starter–generator (ISG), which performs both engine cranking and battery charging, is becoming attractive for modern automobiles and HEVs [9]–[10]. There are many advantages and functions of ISG, some of which are listed below.

• The ISG control can start the engine within 200 ms (compared to 800 ms with dc starter motor) [1]. It imparts an automatic stop/start capability to the engine. This allows the engine to shut down and avoid idling whenever the vehicle is stationary (also known as idle stop by some automotive manufactures) and restart quickly in response to the throttle pedal. This offers major savings in the fuel consumption (typically 10% to 25%) and reduction in the emissions of (carbon dioxide).

• Additional high torque can be provided by the electric machine to the integrated circuit (IC) engine during acceleration (known as "power boost" or "electrical assist"). This allows the use of smaller, more-efficient internal combustion engines. Due to this feature ISG based engines are sometimes termed as mild hybrid.

In order to reduce pollution further we need to bring the engine to idle speed as earliest. On the other hand in order to claim the vehicle as Mild Hybrid Vehicle ISG need to provide torque assistance during high acceleration conditions. In order to perform the both functions we need to extend the torque speed characteristics of ISG. In recent years, various types of electric machines have been utilized as ISG for automobiles and HEVs. The brushless DC (BLDC) Machine is one of the main candidates due to its high efficiency, high power density and wide range speed controllability. Several methods were proposed in literature [2]-[10] to achieve high speed operation of ISG. High speed operation could be achieved by any of the four schemes. The first method is to design the electromagnets in such a way that, the machine possess low back emf which offers high speed for a given system voltage [4]. But the disadvantage is that a low back emf constant results in low starting torque to crank the engine. The second method is winding method i.e., a series winding start and parallel winding run to run the motor at high speed with large starting torque [5], this requires additional switching devices and more complex control logic.

The third method is to use a higher dc bus voltage, where a high starting torque with high speed operation can be achieved. But this scheme has two problems. In normal vehicles at idle engine speed ISG works as generator, but here we are applying higher voltage so at idle engine speed it will not act as generator. In normal vehicles electrical loads are designed for 12V, if we are using higher voltage we need to use separate DC/DC converter for vehicle loads, it will add extra cost weight and space. In this paper a novel low cost converter is proposed to extend the torque speed characteristics of ISG using high voltage batteries without DC/DC converter.

II INTEGRATED STARTER GENRATOR (ISG) MODES

The basic functional block diagram of ISG is shown in Fig. 3. An ISG system typically contains a battery pack, a power converter, an electric machine, and controller for controlling ISG operation. The electric bus voltage is fixed to 12V.
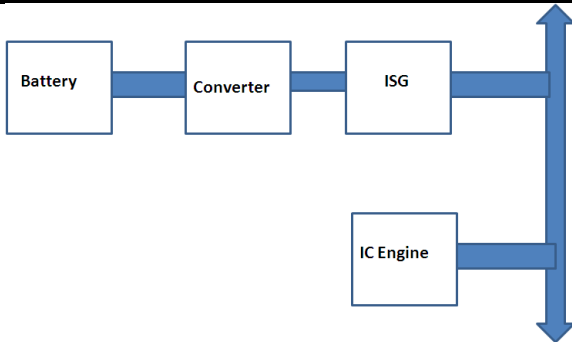
Figure. 1 ISG System

The ISG has four modes of operation. The changeover between different modes depends on operating conditions. At one time it can work in only one mode. The power flow in different modes of operation is shown in Fig. 4. The description of different modes is given below.
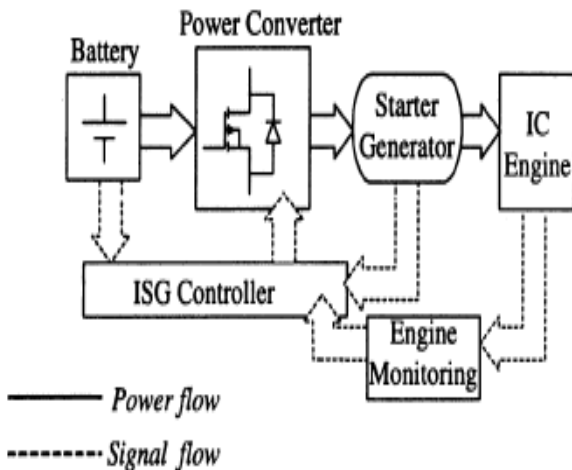

Figure. 2 Power Flow in ISG System during Mode 1 and 4

A. Mode 1:—Engine cranking mode

ISG operates in this mode, when the ignition switch is in the start position. Engine cranking mode is in effect when the engine speed is in between 0–150 rpm. During this mode ISG will provide sufficient torque to start the engine. Once the diesel engine fires the system accelerates; the control then transfers to one of the other modes.

B. Mode 2:—Running power generation mode

Once the engine has taken control over the system, ISG operation enters into power generation mode. In this mode the induction machine extracts power from the crankshaft and recharges the battery such that the bus voltage is maintained at 12 V, irrespective of the load on the bus.

C. Mode 3:—Braking power generation mode

ISG control enters this mode, when the engine brake is ON. It checks for the battery voltage. If the battery voltage is below 12 V, then control operates in power generation mode and extracts maximum power from the engine and charges the battery. If the battery voltage is above 12 V,

then the ISG control enters into power dissipation mode. The power extracted is directed to power grid array to dissipate the energy.
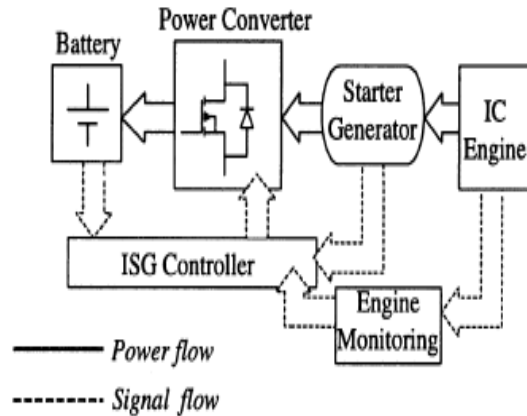

Figure. 3 Power Flow in ISG System during Mode 2 and 3

D. Mode 4:—Power boost mode

ISG operates in the power boost mode, when the engine is running at low speeds (from 600–1000 rpm) and there is high acceleration demand (when the acceleration pedal is greater than 75% and the battery capacity greater than 50% of the rated capacity). In this mode, the induction machine will provide additional torque to the crankshaft to assist in acceleration.

III PROPOSED NOVEL CONVERTER

A Conventional ISG System

Fig. 4 shows the conventional ISG system. In order to extend the torque speed characteristics of ISG a high voltage battery along with DC/DC converter is used. Here DC/DC converter has to be designed for peak power of electrical loads. This will add extra cost weight and space.
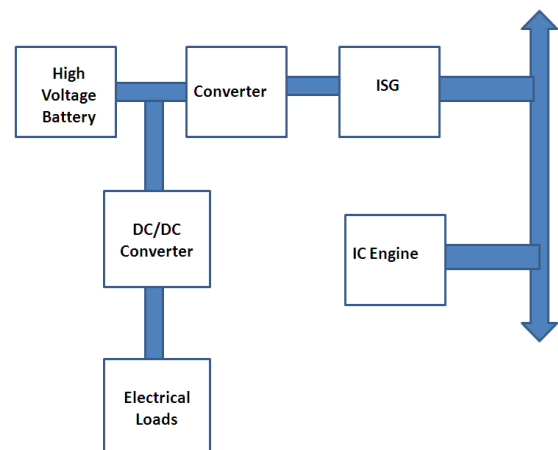

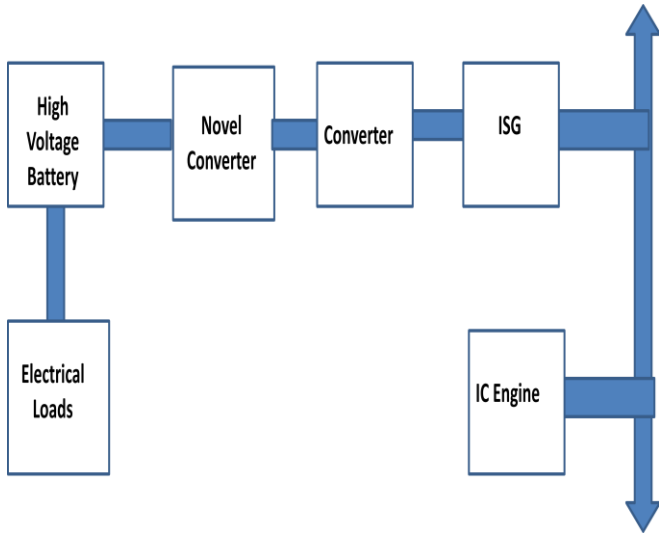Figure. 4 Conventional ISG System

B Proposed ISG System

Figure. 5 Proposed ISG System

Fig. 5 shows the Proposed ISG system. In order to extend the torque speed characteristics of ISG a high voltage battery along with Novel converter is used. The novel converter consists of switches only so the cost of proposed system is lesser than conventional system.

C Proposed Novel Converter

The proposed Novel converter is shown in Fig. 6 It consists of two cascaded half Bridges. By closing switches S1 and S4 we can apply Vdc voltage to ISG. By closing switches S2 and S4 we can apply 2Vdc voltage to ISG. Ths switching table is shown in Table I.
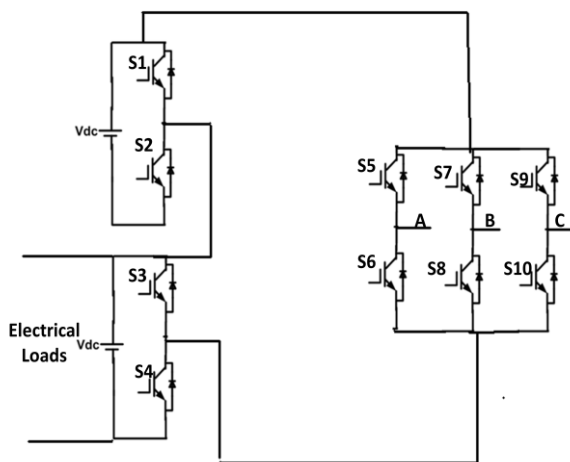

Figure. 6 Proposed Novel Converter

Table 1. Switching table

Switches Turn ON	Voltage Level
S1,S4	Vdc
S2,S4	2Vdc
S2,S3	Vdc

D. Mathamatical Modeling of BLDC

The three phase star connected BLDC motor can be described by the following four equations in bipolar mode of operation.

$$V_{ab} = R(i_a - i_b) + L\frac{d}{dt}(i_a - i_b) + e_a - e_b \dots\dots\dots\dots (1)$$

$$V_{bc} = R(i_b - i_c) + L\frac{d}{dt}(i_b - i_c) + e_b - e_c \dots\dots\dots\dots (2)$$

$$V_{ca} = R(i_c - i_a) + L\frac{d}{dt}(i_c - i_a) + e_c - e_a \dots\dots\dots\dots (3)$$

$$T_e = B\omega_n + j\frac{d\omega_n}{dt} + T_L \dots\dots\dots\dots (4)$$

The symbol v , i and e denote the phase to phase voltages, phase currents and phase back EMF's respectively, in three phases a, b and c. The resistance R and the inductance L are per phase values and T_e and T_L are the electrical torque and the load torque. J is the rotor inertia, B is a friction constant and W_m is the rotor speed. The back EMF's and the electrical torque can be expressed as above

$$e_a = \frac{K_e}{2}\omega_m F(\theta_e) \dots\dots\dots\dots (5)$$

$$e_b = \frac{K_e}{2}\omega_m F\left(\theta_e - \frac{2\pi}{3}\right) \dots\dots\dots\dots (6)$$

$$e_c = \frac{K_e}{2}\omega_m F\left(\theta_e - \frac{4\pi}{3}\right) \dots\dots\dots\dots (7)$$

$$T_e = \frac{k_t}{2}\left[F(\theta_e)i_a + F\left(\theta_e - \frac{2\pi}{3}\right)i_b + F\left(\theta_e - \frac{4\pi}{3}\right)i_c\right] \dots\dots\dots\dots (8)$$

IV Design of Proposed Novel Hybrid H-Bridge Inverter

A Device Current

The IGBT and DIODE currents can be obtained from the load current by multiplying with the corresponding duty cycles. Duty cycle, d = ½(1+Kmsinωt)

![IJEEE logo]

International Journal of Ethics in Engineering & Management Education
Website: www.ijeee.in (ISSN: 2348-4748, Volume 1, Issue 6, June 2014)

Where, m = modulation index K = +1 for IGBT, -1 for Diode.

$$i_{ph} = \sqrt{2}\, I\, \sin(\omega t - \emptyset)$$

Where i = RMS value of the load (output) current,
Ø = Phase angle between load voltage and current.
Then the device current can be written as follows.

$$\therefore\ i_{device} = \frac{\sqrt{2}}{2} I \sin(\omega t - \emptyset) * (1 + km \sin \omega t)$$

The average value of the device current over a cycle is calculated as

$$i_{avg} = \frac{1}{2\pi} \int_{\emptyset}^{\pi+\emptyset} \frac{\sqrt{2}}{2} I \sin(\omega t\text{-}\emptyset)*(1 + k\, m\sin\omega t)d\omega t$$

$$= \sqrt{2}\, I \left[\frac{1}{2\pi} + \frac{K\,m}{8} \cos\emptyset\right]$$

The device RMS current can be written as

$$i_{rms}$$

$$= \sqrt{\int_{\emptyset}^{\pi+\emptyset} \frac{1}{2\pi}\left(\sqrt{2}\, I \sin(\omega t - \emptyset)\right)^2 * \frac{1}{2} * \left((1 + k\, m\sin\omega t)d\omega t\right)}$$

$$= \sqrt{2}\, I \sqrt{\left[\frac{1}{8} + \frac{K\,m}{3\pi}\cos\emptyset\right]}$$

B   IGBT Loss Calculation

IGBT loss can be calculated by the sum of switching loss and conduction loss. Where conduction loss can be calculated by,

$$P_{on(IGBT)} = V_{ceo} * I_{avg(igbt)} + I_{rms(igbt)}^2 * r_{ceo}$$

$$I_{avg(igbt)} = \sqrt{2}\, I \left[\frac{1}{2\pi} + \frac{m}{8}\cos\emptyset\right]$$

$$I_{rms(igbt)} = \sqrt{2}\, I \sqrt{\left[\frac{1}{8} + \frac{m}{3\pi}\cos\emptyset\right]}$$

Values of V_{ceo} and r_{ceo} at any junction temperature can be obtained from the output characteristics (Ic vs. Vce) of the IGBT as shown in Fig .7.
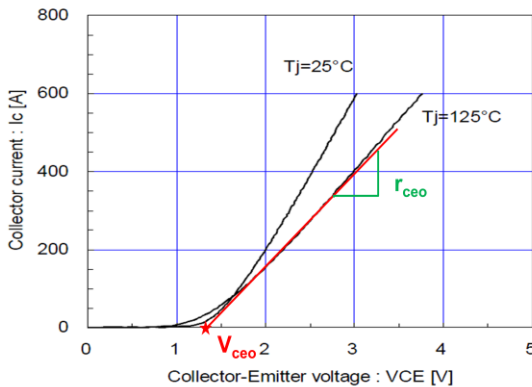

Figure 7 IGBT output characteristics

The switching losses are the sum of all turn-on and turn-off energies at the switching events

$$E_{sw} = E_{on} + E_{off} = a + b\, I + c\, I^2$$

Assuming the linear dependence, switching energy $E_{sw} =$

$$(a + b\, I + c\, I^2) * \frac{V_{DC}}{V_{nom}}$$

Here V_{DC} is the actual DC-Link voltage and V_{nom} is the DC-Link Voltage at which E_{sw} is given. Switching losses are calculated by summing up the switching energies.

$$P_{sw} = \frac{1}{T_o} \sum_n E_{sw}(i)$$

Here 'n' depends on the switching frequency.

$$P_{sw} = \frac{1}{T_o} \sum_n (a + b\, I + c\, I^2)$$

$$= \frac{1}{T_o}\left[\frac{a}{2} + \frac{b\, I}{\pi} + \frac{c\, I^2}{4}\right]$$

After considering the DC-Link voltage variations switching losses of the IGBT can be written as follows.

$$P_{sw(IGBT)} = f_{sw}\left[\frac{a}{2} + \frac{b\, I}{\pi} + \frac{c\, I^2}{4}\right] * \frac{V_{DC}}{V_{nom}}$$

So, the sum of conduction and switching losses gives the total losses.

$$P_{T(IGBT)} = P_{on(IGBT)} + P_{sw(IGBT)}$$

C   Diode Loss Calculation

The DIODE switching losses consists of its reverse recovery losses and the turn-on losses are negligible.

$$E_{rec} = a + b\, I + c\, I^2$$

$$P_{sw(DIODE)} = f_{sw}\left[\frac{a}{2} + \frac{b\, I}{\pi} + \frac{c\, I^2}{4}\right] * \frac{V_{DC}}{V_{nom}}$$

So, the sum of conduction and switching losses gives the total DIODE looses.

$$P_{T(DIODE)} = P_{on(DIODE)} + P_{sw(DIODE)}$$

The total loss per one switch (IGBT+DIODE) is the sum of one IGBT and DIODE loss.

$$P_T = P_{T(IGBT)} + P_{T(DIODE)}$$

D.   Thermal Calculations

The junction temperatures of the IGBT and DIODE are calculated based on the device power losses and thermal resistances. The thermal resistance equivalent circuit for a module is shown in Fig 8. In this design the thermal calculations are started with heat sink temperature as the reference temperature. So, the case temperature from the model can be written as follows.

$$T_c = P_T R_{th(c-h)} + T_h$$

Here $R_{th(c-h)}$ = Thermal resistance between case and heat sink

$$P_T = \text{Total Power Loss (IGBT+DIODE)}$$

IGBT junction temperature is the sum of the case temperature and temperature raise due to the power losses in the IGBT.

$$T_{j(IGBT)} = P_{T(IGBT)} R_{th(j-c)IGBT} + T_c$$

DIODE junction temperature is the sum of the case temperature and temperature raise due to the power losses in the DIODE.

$$T_{j(DIODE)} = P_{T(DIODE)} R_{th(j-c)DIODE} + T_c$$

The above calculations are done based on the average power losses computed over a cycle. So, the corresponding thermal calculation gives the average junction temperatures. In order to make the calculated values close to the actual values, transient temperature values are to be added to the average junction temperatures.
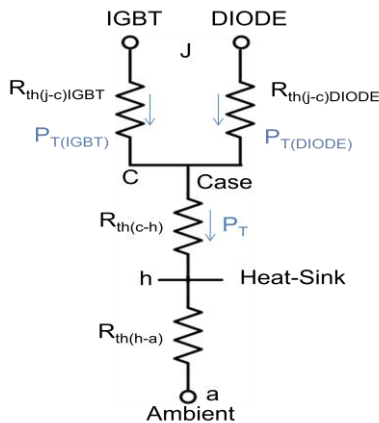

Figure. 8 Thermal resistance equivalent circuit

V MATLAB/SIMULINK MODELING AND SIMULATION RESULTS

Fig. 9 shows the Matlab/Simulink model of Proposed ISG system with novel converter.
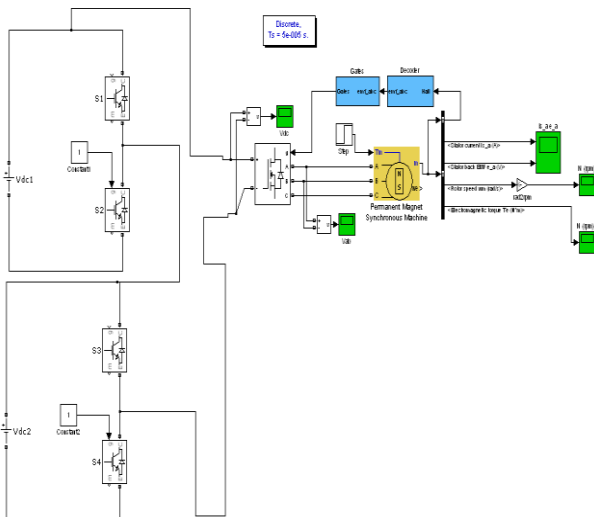

Figure. 9 Matlab/Simulin k M\model of Proposed Novel Converter

Fig. 10 and Fig. 11 shows the torque and speed when battery one is connected. The final attained speed is 1500 rpm.
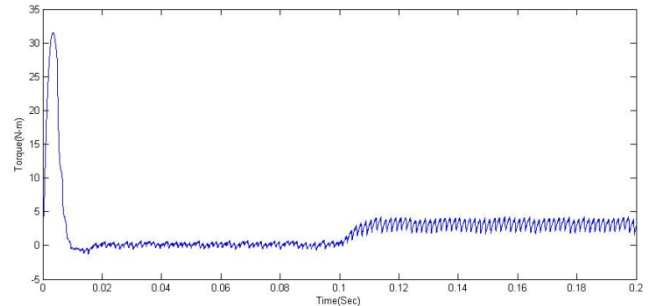

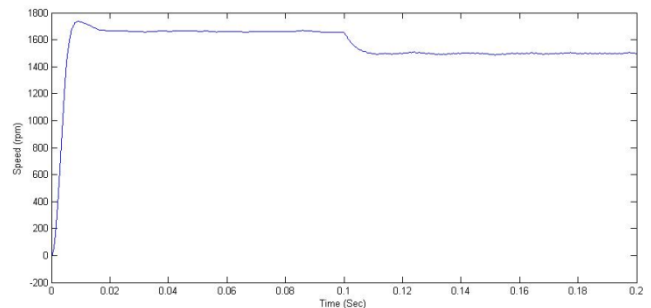Figure. 10 Torque when one battery is connected

Figure. 11 Speed when one battery is connected

Fig.12 and Fig. 13 shows the torque and speed when both batteries are connected. The final attained speed is 3000 rpm. During generator mode each battery is connected across the machine for a fixed time. This will eliminates the charging problem during engine idle speed.
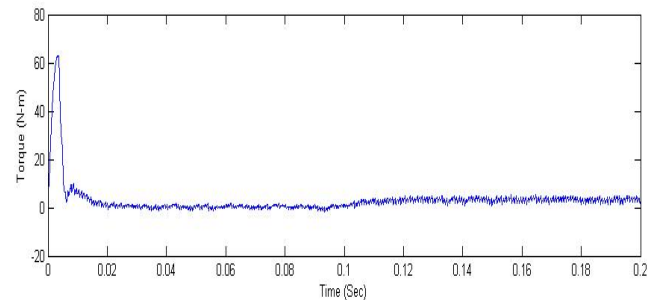

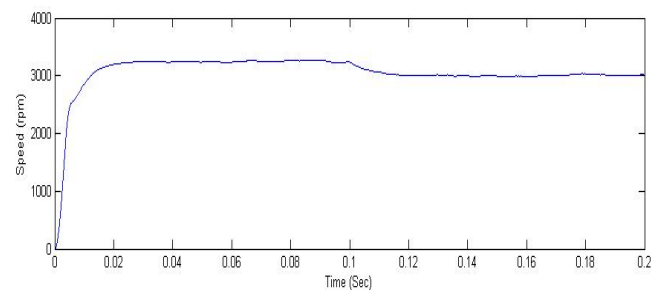Figure. 12 Torque when two batteries are connected

Figure. 13 Speed when two batteries are connected

VI CONCLUSION

In this paper a novel low cost converter is proposed to extend the torque speed characteristics of Integrated Starter Generator (ISG). The proposed converter uses only four additional switches compared to conventional ISG system with DC/DC converter. It will reduce cost space and complexity. Finally Matlab/Simulink based model is developed and simulation results are presented.

REFERENCES

[1]. J. G. Kassakian, J. M. Miller, and N. Traub, "Automotive power electronics up," *IEEE Spectrum Mag.*, pp. 34–39, May 2000.

[2]. J. G. Kassakian, "Automotive electrical systems—the power electronics market of the future," in *Proc. IEEE Appl. Power Electron. Conf.*, 2000, vol. 1, pp. 3–9.

[3]. SAE, "Transition to 42-Volt Electrical System," Tech. Rep. SP-1556, Society for Automotive Engineers May 2000.

[4]. C. Williams, "Comparison and review of electric machines for integrated starter generator applications," in *Proc. IEEE 39th IAS Annu. Meeting, Conf.*, Oct. 3–7, 2004, vol. 1, pp. 386–396.

[5]. P. J. McCleer, J.M.Miller, A. R. Gale, M. W. Degner, and F. Leonardi, "Nonlinear model amd momentary performance capability of cage induction machine used for combined ISA," *IEEE Trans. Ind. Appl. Soc.*,vol. 37, no. 3, pp. 840–846, May/Jun. 2001.

[6]. H. Rehman, X. Xu, N. Liu, G. S. Kahlon, and R. J. Mohan, "Induction machine drive system for Visteon integrated starter-alternator," in *Proc.IEEE IECON'99*, Nov. 29–Dec. 3 1999, vol. 2, pp. 636–641.

[7]. M. Naidu and J. Walters, "A 4 KW, 42 V induction machine based power generation system with a diode bridge rectifier and a PWM inverter," *IEEE Trans. Ind. Appl.*, vol. 39, no. 5, pp. 1287–1293, Sep./Oct.2003.

[8]. S. Chen, B. Lequesne, R. R. Henry, Y. Xue, and J. J. Ronning, "Design and testing of belt driven induction starter-generator," *IEEE Trans. Ind. Appl.*, vol. 38, no. 6, pp. 1525–1533, Nov./Dec. 2002.

[9]. I. Takahashi and T. Noguchi, "A new quick response and high efficiency control strategy of induction machine," *IEEE Trans. Ind. Appl.*,vol. IA-2, no. 5, pp. 820–827, Sep./Oct. 1986.